A High-k_t^2 Switchable Ferroelectric $Al_{0.7}Sc_{0.3}N$ Film Bulk Acoustic Resonator

Jialin Wang*, Mingyo Park*, Stefan Mertin**, Tuomas Pensala**, Farrokh Ayazi*, and Azadeh Ansari*

* School of Electrical and Computer Engineering
Georgia Institute of Technology
Atlanta GA, USA

**VTT Technical Research Centre of Finland

Espoo, Finland

***Abstract*—This work demonstrates the hysteresis behavior and temperature characterization of an AlScN Film bulk acoustic resonator (FBAR) with ~30% Sc/(Al+Sc) ratio. Operating at ~3 GHz, the as-fabricated FBAR exhibits a record high effective electromechanical coupling (k_t^2) of 18% with a mechanical quality factor (Q_m) of 328. The polarization of the FBAR can be switched from N-polar to Al-polar by using a triangular-wave signal with a peak voltage of −350 V, applied for 6 seconds at 1 kHz across a 900 nm-thick $Al_{0.7}Sc_{0.3}N$ film. It is shown that the polarization switching of AlScN film not only changes the polarity of the piezoelectric coefficient (e_{33}), but also changes the series resistance of the metal-ferroelectric-metal (MFM) stack and leads to an effective "switching" of the FBAR. The frequency response of the switchable FBAR is investigated after polarization switching during 4 cycles and at elevated temperatures up to 600 K.**

Keywords – ***Ferroelectric; Acoustic resonators; Filters; FBAR; Aluminum Scandium Nitride; Frequency tuning; Piezoelectric films***

I. INTRODUCTION

Increasing the Sc content (x) in $Al_{1-x}Sc_xN$ films, has shown to increase the piezoelectric response as compared to pure AlN films. A boost of up to 5× in piezo-response was measured for AlScN films with up to 40% Sc/(Al+Sc) ratios [1,2]. This boost will result in improvement of the effective electromechanical coupling coefficient (k_t^2) in AlScN resonators, translating into larger fractional bandwidths in acoustic filters.

Recently, Fichtner *et al.* reported on the ferroelectric properties of AlScN films with Sc/(Al+Sc) ratios above 27%. [3]. The recently discovered ferroelectric behavior, together with the excellent piezoelectric properties, and the CMOS-compatibility of sputtered films, makes AlScN a promising candidate as a multi-functional material for reconfigurable filters.

II. RESULTS AND DISCUSSION

The resonant stack consists of Mo/$Al_{0.7}Sc_{0.3}N$/Mo thin films with the stack thickness of 100/900/100 nm. The entire stack is sputter-deposited on an SOI substrate at the VTT Technical Research Centre of Finland. FBARs are fabricated at the Georgia Tech clean room facilities, as detailed in Ref. [4].

Figure 1(a) shows the hysteresis P-E curve of $Al_{0.7}Sc_{0.3}N$ film. The remnant polarization of the film reaches up to 80 μC/cm^2 with asymmetric coercive field around 3.5 MV/cm. Compared to PZT, the PE loop of AlScN film has two clearly defined states (box-like loop), and a very low leakage current [3]. The box-like P-E loop is measured with a modified S-T circuit shown in figure 1(b) [5]. The cross-section of the sample taken from SEM shown in figure 1(c) reveals a textured film growth. X-ray diffraction, performed with Panalytical Xpert Por MRD XRD, confirmed a pure c-axis orientation of AlScN thin film in AlN wurtzite structure. The rocking curve (ω-θ) measurement shows an FWHM value of 2.05° (figure 1(d)). Figure 2 shows the measured and mBVD-fitted model of admittance frequency response (Y11 (dB)) and the Smith chart representation of the FBAR device at the two different states (before and after polarization switching). The switching of the FBAR is achieved by applying a unipolar triangle-wave with −350 V peak voltage at 1 kHz for 6 s (figure 2(d)). The application of the −350 V voltage causes a polarization switch and is then removed when the FBAR frequency response is measured in figure 2(d). It must be noted that no significant change was observed in the frequency and phase response of the FBAR at switching voltages below −350 V. The durability of FBAR is studied by switching between the two states by applying −350 V and +350 V sequentially. Figure 3 shows the result of this test; the FBAR could switch between positive and negative biases; however, the device shows performance degradation as the number of switching cycles increases. The k_t^2 of the FBAR is calculated using Eq. 1 [6] as 18 %, which is among the highest k_t^2 values reported for AlN-based resonators to date [7-10]. The FBAR maintains a Q_{bode} of 213 at f_p and an unloaded (mechanical) Q_m of 328, extracted by mBVD model (Fig. 2(a) and (b)). Table I shows the extracted parameters of the mBVD model used to calculate Q_m.

Table I. Extracted parameters of the mBVD model.

Rs (Ω)	Rm (Ω)	Lm (nH)	Cm (fF)	Co (fF)	Ro (Ω)	k_t^2 (%)	*Qm*
3.67	0.34	6.09	488	2660	2225	18.2	328

The FBAR is switched by applying -350V bias, as shown in figures 2(a) and (b). The series frequency (f_s) of the FBAR switches off after -350V bias is applied and removed, which is attributed to the resistance switching at two polarization states, similar to resistive switching observed in other metal-

This work was supported by the National Science Foundation (ECCS-1542174) and National Science Foundation CAREER Award (ECCS-1944304).

978-1-7281-6430-4/20/$31.00 ©2020 IEEE

ferroelectric-metal (MFM) capacitors [11-15]. Similar to the static electrical branch of the mBVD model shown in figure 2(e), the MFM capacitor can be modeled with a series resistor (R_s), which represents the metal electrode resistance and the resistance between the metal/ferroelectric material interface; and a parallel ferroelectric resistor (R_{FE}), and a capacitor (C_{FE}) (represented as R_o and C_o in the mBVD model). The switching bias can cause a change in R_s and R_{FE}, depending on the applied stress. Previous studies have shown that the polarization inversion of the ferroelectric layer could cause an increase in the energy barrier height of metal/ferroelectric interface, which then leads to an increase in the series resistance (R_s) [12,13,15]. The switching of the FBAR series resonance frequency in this work (figure 2(a,b)) is attributed to the 20× increase of R_s, when the bias voltage is applied for 6s.

The temperature-dependent P-E measurements, as well as the temperature coefficient of frequency (TCF) characterization of the series and parallel resonance frequencies (f_s and f_p) are shown in figure 4. Figure 4(a) shows that the P-E loop shrinks at high temperatures and the coercive field drops to ~1.60 MV/cm, at 600 K [16]. Operation at elevated temperature can lower the required ferroelectric switching voltage. The TCF of the FBAR is measured as -39.6 ppm/k for f_s.

$$k_t^2 = \frac{\pi^2}{4}\left(f_p - f_s\right) \times \frac{f_s}{f_p^2} \text{ [6]} \qquad (1)$$

III. CONCLUSIONS

This work marks the first demonstration of $Al_{0.7}Sc_{0.3}N$ ferroelectric FBARs, with a record high effective electromechanical coupling coefficient (k_t^2) of 18.1%. We also demonstrated for the first time the temperature characterization of hysteresis and frequency response of $Al_{0.7}Sc_{0.3}N$ ferroelectric FBARs at temperatures up to 600 K. Furthermore, the FBARs were switched between two polarization states upon application of triangular waveforms with a peak voltage of -350 V and +350 V at 1 kHz and for 6 s. Application and removal of the switching bias caused a 20 × change in the series resistance of the MFM capacitor, besides switching the polarity of e_{33} piezoelectric coefficient value of the AlScN film. Such R_s switching enabled an "intrinsically switchable" FBAR, that can be used as the building block of wideband reconfigurable acoustic filters.

ACKNOWLEDGMENT

The sputtered piezo-stack $Mo/Al_{0.7}Sc_{0.3}N/Mo$ was provided by VTT Technical Research Centre of Finland. The FBAR devices were fabricated at the Institute for Electronics and Nanotechnology (IEN) cleanroom facility at the Georgia Institute of Technology, a member of the National Nanotechnology Coordinated Infrastructure (NNCI), which is supported by the National Science Foundation (Grant ECCS-1542174). This work is supported by NSF CAREER award (ECCS-1944304).

REFERENCES

[1] A. Teshigahara, K. Hashimoto and M. Akiyama, "Scandium aluminum nitride: Highly piezoelectric thin film for RF SAW devices in multi GHz range," *2012 IEEE International Ultrasonics Symposium*, Dresden, 2012

[2] M. Park and S. Kim, "Thermal conductivity of AlN thin films deposited by RF magnetron sputtering," *Materials Science in Semiconductor Processing*, vol. 15, Issue 1, 2012, Pages 6-10. DOI: https://doi.org/10.1016/j.mssp.2011.04.007.

[3] S. Fichtner, N. Wolff, F. Lofink, L. Kienle, and B. Wagner, "AlScN: A III-V semiconductor based ferroelectric," *Journal of Applied Physics* 125, 114103, 2019. DOI: https://doi.org/10.1063/1.5084945.

[4] J. Wang, M. Park, S. Mertin, T. Pensala, F. Ayazi, A. Ansari, "A Film Bulk Acoustic Resonator based on Ferroelectric Aluminum Scandium Nitride Films", in *Journal of Microelectromechanical Systems* (Accepted)

[5] Sawyer C Band Tower C H "Rochelle salt as a Dielectric," *Phys. Rev*. 35 269, 1930.

[6] H. Igeta, M. Totsuka, M. Suzuki and T. Yanagitani, "Temperature Characteristics of ScAlN/SiO2 BAW Resonators," *2018 IEEE International Ultrasonics Symposium (IUS)*, Kobe, 2018, pp. 1-4.doi: 10.1109/ULTSYM.2018.8580165.

[7] H. Campanella, "Characterization Techniques", in *Acoustic wave and electromechanical resonators: concept to key applications*. Boston: Artech House, Boston USA, 2010, pp, 127-158.

[8] T. Yanagitani and M. Suzuki, "Electromechanical coupling and gigahertz elastic properties of ScAlN films near phase boundary," *Appl. Phys. Lett.* 105, 2014. DOI: https://doi.org/10.1063/1.4896262

[9] K. Umeda, H. Kawai, A. Honda, M. Akiyama, T. Kato and T. Fukura, "Piezoelectric properties of ScAlN thin films for piezo-MEMS devices," *2013 IEEE 26th International Conference on Micro Electro Mechanical Systems (MEMS)*, Taipei, 2013

[10] M, Schneider, M. DeMiguel-Ramos, A.J Flewitt, E. Iborra, and U. Schmid, "Scandium Aluminium Nitride-Based Film Bulk Acoustic Resonators." *Proceedings* 2017, DOI: 10.3390/proceedings1040305.

[11] Z. Yan, and J. Liu "Resistance switching memory in perovskite oxides," *Annals of Physic*s, 2015. DOI: https://doi.org/10.1016/j.aop.2015.03.028

[12] B. Tian, Y. Liu, L. Chen, J. Wang, S. Sun, H. Shen, J. Sun, G. Yuan, S. Fusil, V. Garcia, B. Dkhil, X. Meng, and J. Chu, "Space-charge effect on electroresistance in metal-ferroelectric-metal capacitors," *Scientific Reports 5,* 2016, DOI: https://doi.org/10.1038/srep18297.

[13] P. Lopez-Varo, L. Bertoluzzi, J. Bisquert, M. Alexe, M. Coll, J. Huang, J. Jimenez-Terjada, T. Kirchartz, R. Nechache, F. Rosei, and Y. Yuan, "Physical aspects of ferroelectric semiconductors for photovoltaic solar energy conversion," *Physics Reports,* Volume 653, 2016, DOI: https://doi.org/10.1016/j.physrep.2016.07.006.

[14] R. Meyer, J.R. Contreras, A. Petraru, and H. Kohlstedt, "On a novel ferro resistive random access memory (FRRAM): basic model and first experiments, integrated ferroelectrics," *Integrated Ferroelectrics,* Volume 64, 2004, DOI: https://doi.org/10.1080/10584580490893655.

[15] J.E. Rault, T. Maroutian, G. Agnus, Ph. Lecoeur, G. Niu, M.G. Silly, B. Vilquin, A. Bendounan, F. Sirotti, and N. Barrett, "Interface electronic structure in a metal/ferroelectric heterostructure under applied bias," *Physical Review B.* Volume 87, 2013, DOI: 10.1103/PhysRevB.87.155146.

[16] Y. Zhang, Z. Chen, W. Cao, Z, Zhang, "Temperature and frequency dependence of the coercive field of 0.71PbMb 1/3 Nb 2/3 O 3 –0.29PbTiO 3 relaxor-based ferroelectric single crystal, "*Applied Physics Letters*. 2017, doi: 172902. 10.1063/1.4998187.

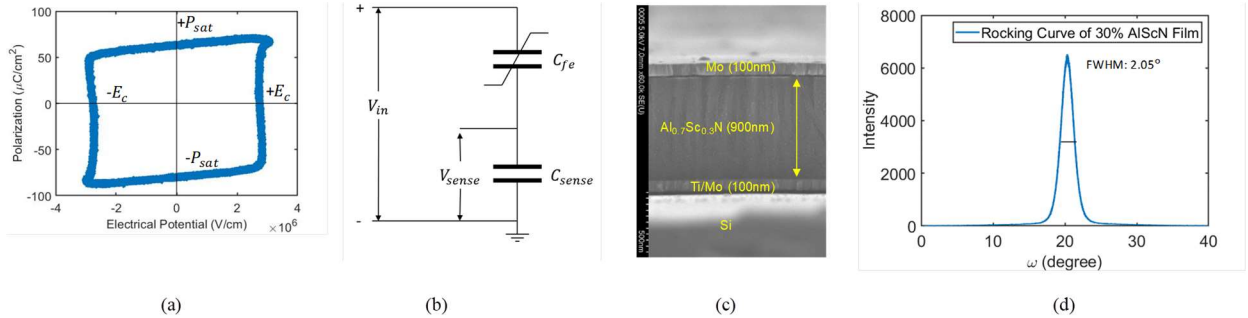

(a) (b) (c) (d)

Figure 1. *(a) P-E loop of sputtered AlScN thin film with Sc/(Al+Sc) ratio of 30%. (b) S-T circuit diagram for P-E loop measurement (c) SEM cross-sectional image of the thin film (d) Rocking-curve measurement of the (002) AlScN peak*

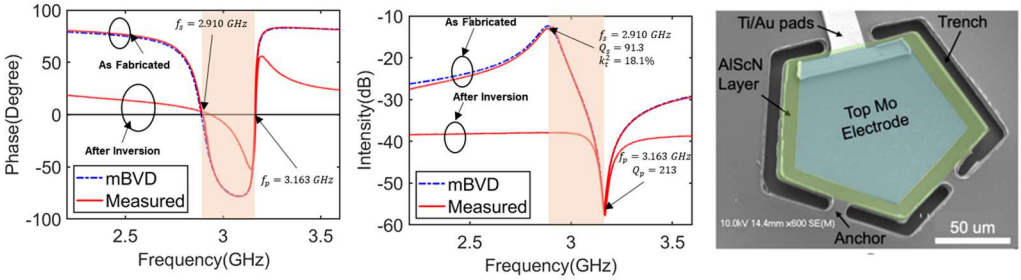

(a) (b) (c)

Figure 2. *(a) Admittance magnitude Y11 (dB) before and after inversion for both measured and mBVD-fitted model (b) Phase of Y11, showing f_s and f_p of 2.910 and 3.163 GHz, resulting in k_t^2 of 18%. (c) SEM image of FBAR. (d) Waveform of the switching bias signal. (d) Unipolar waveform used in this work for switching the polarization of the ferroelectric film. (e) modified Butterworth-Van Dyke (mBVD) circuit model*

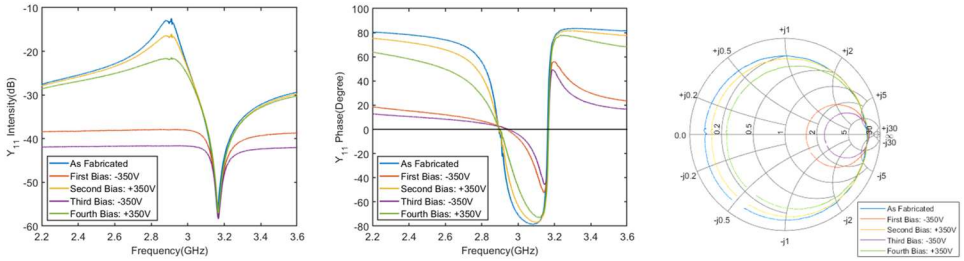

(a) (b) (c)

Figure 3. *(a) Magnitude and (b) phase of FBAR admittance with multiple switching cycles with positive and negative polarities. (c) Smith Chart representation of the FBAR with multiple switching cycle with frequency between 2.2 to 3.6 GHz, showing performance degradation after each cycle.*

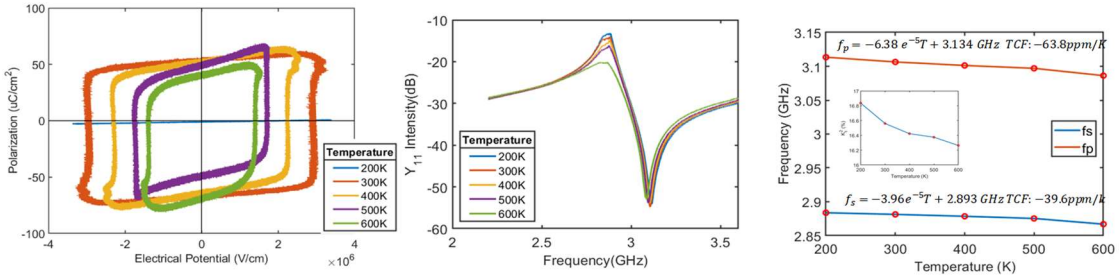

(a) (b) (c)

Figure 4. *Thermal characterization of (a) MFM capacitor PE loops at a temperature range of 200 to 600K, (b) FBAR admittance frequency response, and (c) f_p, f_s, and k_t^2 vs. temperature.*